A New Current Model Flux Observer for Wide Speed Range Sensorless Control of an Induction Machine

Habib-ur Rehman, *Member, IEEE,* Adnan Derdiyok, Mustafa K. Guven, *Member, IEEE,* and Longya Xu, *Senior Member, IEEE*

***Abstract*—A new close loop current model flux observer is designed to estimate the rotor flux, position and velocity of an induction machine. The current observer includes carefully designed sliding mode functions which are derivative of the fluxes along the α and β axes. Therefore, when the estimated current converges to the measured one, the flux estimation is a mere integration of the sliding mode function. The rotor speed can then be derived from the sliding mode functions and the estimated flux. In the current and flux observers all of the terms that contain the rotor time constant and the rotor speed have been replaced by the sliding mode functions, thus making the proposed current and flux estimations completely insensitive to the rotor time constant variation and any error in the estimated speed. Simulations and experiments are performed under a variety of conditions to validate the effectiveness of the proposed algorithm.**

***Index Terms*—Current model flux observer, induction machine, sensorless control, sliding mode.**

I. Introduction

METHODS to estimate the flux, rotor position and velocity of an induction machine for sensorless control have been extensively studied in the past two decades. Two main directions for these estimations are

a) rotor saliency based on signal injection [1]–[8];
b) terminal quantities based on measurements of stator voltages and currents [9]–[26].

The saliency based technique with the fundamental excitation [1], [2] often fails at low and zero speeds. When applied with the high frequency signal injection [3]–[8], the method may cause torque ripples, vibration, and audible noise. Also, the saliency based technique is machine specific and can not be applied to a standard machine. Therefore, the focus of this paper is flux, rotor position and velocity estimation based on terminal quantities [9]–[26].

The key issues when using the terminal quantity method are flux integration, unavailability of the signal at low speed and parameter sensitivity. The voltage model flux observer is especially sensitive to the stator resistance at low speed and the leakage inductance at all speeds. The current model flux observer is sensitive to the rotor time constant, which varies with the temperature. Also an error in the estimated speed will affect the flux estimation because the flux estimation in the current model flux observer requires the rotor speed information. Different schemes to overcome these problems and to improve the sensorless control have been proposed in the literature [9]–[26].

The voltage model flux and speed estimations [9] have problems at low frequency regions where the signal to noise ratio of the stator voltage measurement is very poor, and voltage drop on the stator resistance is dominant. The voltage model is also sensitive to the leakage inductance. Xu [10]–[12] used the stator flux orientation in which leakage inductance appears in the feedback loop of the system, and hence improves the system performance as well as steady state operation.

The current model flux observer is considered to out perform the voltage model flux observer at low speeds. Also, its accuracy is relatively unaffected by the leakage inductance for any operating condition [13]. However, it does not work well at high speed due to rotor resistance variation. As a solution, it has been suggested to use the current model observer at low speed and voltage model observer at high speed [13], [14]. To further improve the observers performance, close loop rotor flux observers are proposed. These observers use the estimated stator currant error [13]–[15] or the estimated stator voltage error [15], [16] to drive the estimated rotor flux to the actual flux. Model reference adaptive schemes are proposed in [16]–[18], where one of the flux estimators acts as a reference model, and the other acts as the adaptive estimator. To overcome the integration problem, Tajima [16] and Peng [17] suggested the use of back emf and instantaneous reactive power as alternative ways of forming the errors used to estimate the velocity in the adaptive controller. However, an accurate flux estimation problem still remains. Another problem arises because the rotor velocity adaptation is error driven. This causes an inherent lag in the velocity estimate. Reduced order observers are designed in [19], in which only the rotor flux, not the stator current is estimated. The correction is then applied by using the error between the actual stator voltage vector and an estimate. However, this requires adding voltage sensors to the system, which is not desirable.

Extended Kalman filters have also been proposed [20], [21] as a potential solution for better flux estimation when using the motor terminal quantities alone. Unfortunately, this approach contains some inherent disadvantages such as it's computational expense and have no specific design and tuning criteria.

Sliding mode has been documented to have the advantages of robustness and parameters insensitivity [22]. Flux observers

Manuscript received May 23, 2002; revised August 1, 2002. Recommended by Associate Editor J. Ojo.

H.-u. Rehman is with the Department of Electrical Engineering, United Arab Emirates University, Al-ain, United Arab Emirates (e-mail: hrehman@uaeu.ac.ae).

A. Derdiyok is with the Department of Electronics Engineering, Atatürk University, 25240, Erzurum, Turkey (e-mail: derdiyok@atauni.edu.tr).

M. K. Guven is with Caterpillar, Inc., Technical Center E-855, Peoria, IL 61656-1875 USA (e-mail: guven_mustafa_k@cat.com).

L. Xu is with Ohio State University, Columbus, OH 43210 USA (e-mail: xu@ee.eng.ohio-state.edu).

Digital Object Identifier 10.1109/TPEL.2002.805579

have been designed [22]–[26] using the sliding mode technique for sensorless speed control of induction machines. These algorithms use a current model flux observer and apply a correction term based on the current estimation error. The performance of sliding mode observer presented in [22], [23] is experimentally validated for sinusoidal speed tracking with limited band width capability. Also, all of these observers [22]–[26] require the rotor speed and rotor time constant for the current and flux estimations. Therefore, an error in the estimated speed or rotor time constant will affect the current and flux estimations, and thus degrade the observer accuracy.

In this paper, a new current model flux observer is developed, with the goal of not requiring any speed and rotor time constant information. Therefore, any error in the rotor time constant and estimated speed will not be fed back into the current or flux estimations, a feature widely different from the current model flux observers designed to date. The inherited qualities of the sliding mode control, coupled with the way this observer is designed, will result in a sensorless controller which is invariant to external disturbances and has better dynamic performance over a wide speed range.

II. Methodology for the Proposed Flux and Speed Observers

In this section, first we describe the dynamic model of the induction machine with the stator currents and rotor fluxes. This is commonly known as the current model flux observer. This description is followed by the design of two sliding mode functions along α and β axes, which lead to the proposed new close loop current model flux observer requiring no rotor time constant and rotor speed information. Machine speed is determined using the estimated flux and the sliding mode functions, thus completing the design of proposed current, flux and speed observers.

A. Induction Machine Dynamic Model and the Sliding Mode Functions

The induction machine model with the stator currents and rotor fluxes defined as the state variables can be written in the stationary α–β coordinate system as

$$\begin{aligned}
\dot{I}_{\alpha s} &= \frac{1}{\sigma L_s}\frac{L_m}{L_r}\frac{1}{T_r}\lambda_{\alpha r} + \frac{1}{\sigma L_s}\frac{L_m}{L_r}\omega_r\lambda_{\beta r} \\
&\quad - \frac{1}{\sigma L_s}\left(R_s + \frac{L_m^2}{L_r T_r}\right) I_{\alpha s} + \frac{1}{\sigma L_s} V_{\alpha s}, \\
\dot{I}_{\beta s} &= \frac{1}{\sigma L_s}\frac{L_m}{L_r}\frac{1}{T_r}\lambda_{\beta r} - \frac{1}{\sigma L_s}\frac{L_m}{L_r}\omega_r\lambda_{\alpha r} \\
&\quad - \frac{1}{\sigma L_s}\left(R_s + \frac{L_m^2}{L_r T_r}\right) I_{\beta s} + \frac{1}{\sigma L_s} V_{\beta s}, \\
\dot{\lambda}_{\alpha r} &= -\frac{1}{T_r}\lambda_{\alpha r} - \omega_r\lambda_{\beta r} + \frac{L_m}{T_r} I_{\alpha s}, \\
\dot{\lambda}_{\beta r} &= -\frac{1}{T_r}\lambda_{\beta r} + \omega_r\lambda_{\alpha r} + \frac{L_m}{T_r} I_{\beta s}.
\end{aligned}$$

These equations can be represented in the matrix form as

$$\begin{aligned}
\begin{bmatrix} \dot{I}_{\alpha s} \\ \dot{I}_{\beta s} \end{bmatrix} &= k_1 \left(\begin{bmatrix} \eta & \omega_r \\ -\omega_r & \eta \end{bmatrix} \begin{bmatrix} \lambda_{\alpha r} \\ \lambda_{\beta r} \end{bmatrix} - \eta L_m \begin{bmatrix} I_{\alpha s} \\ I_{\beta s} \end{bmatrix} \right) \\
&\quad - k_2 \begin{bmatrix} I_{\alpha s} \\ I_{\beta s} \end{bmatrix} + k_3 \begin{bmatrix} V_{\alpha s} \\ V_{\beta s} \end{bmatrix}, \qquad (1)
\end{aligned}$$

$$\begin{bmatrix} \dot{\lambda}_{\alpha r} \\ \dot{\lambda}_{\beta r} \end{bmatrix} = -\left(\begin{bmatrix} \eta & \omega_r \\ -\omega_r & \eta \end{bmatrix} \begin{bmatrix} \lambda_{\alpha r} \\ \lambda_{\beta r} \end{bmatrix} - \eta L_m \begin{bmatrix} I_{\alpha s} \\ I_{\beta s} \end{bmatrix} \right). \qquad (2)$$

In (1) and (2)

$$k_1 = \frac{k_3 L_m}{L_r}, \qquad k_2 = \frac{R_s}{\sigma L_s}, \qquad k_3 = \frac{1}{\sigma L_s},$$
$$\sigma = 1 - \frac{L_m^2}{L_s L_r}, \qquad \eta = \frac{1}{T_r} = \frac{R_r}{L_r}.$$

We next define the matrix S as

$$S = \left(\begin{bmatrix} \eta & \omega_r \\ -\omega_r & \eta \end{bmatrix} \begin{bmatrix} \lambda_{\alpha r} \\ \lambda_{\beta r} \end{bmatrix} - \eta L_m \begin{bmatrix} I_{\alpha s} \\ I_{\beta s} \end{bmatrix} \right).$$

It can be observed in (1) and (2) that the matrix S appears as a common term in both the current and flux equations of the machine. By their nature, (1) and (2) have the advantage that the coupling terms between α and β axes are exactly the same. This implies that the coupling terms can be replaced with the same sliding mode function $\psi_{\alpha\beta r}$. On convergence, the sliding mode function will provide an estimate of the matrix S

$$\begin{bmatrix} \psi_{\alpha r} \\ \psi_{\beta r} \end{bmatrix} = \hat{S} = \left(\begin{bmatrix} \eta & \hat{\omega}_r \\ -\hat{\omega}_r & \eta \end{bmatrix} \begin{bmatrix} \hat{\lambda}_{\alpha r} \\ \hat{\lambda}_{\beta r} \end{bmatrix} - \eta L_m \begin{bmatrix} \hat{I}_{\alpha s} \\ \hat{I}_{\beta s} \end{bmatrix} \right). \qquad (3)$$

Therefore, (1) for current observer becomes

$$\begin{bmatrix} \dot{\hat{I}}_{\alpha s} \\ \dot{\hat{I}}_{\beta s} \end{bmatrix} = k_1 \begin{bmatrix} \psi_{\alpha r} \\ \psi_{\beta r} \end{bmatrix} - k_2 \begin{bmatrix} \hat{I}_{\alpha s} \\ \hat{I}_{\beta s} \end{bmatrix} + k_3 \begin{bmatrix} V_{\alpha s} \\ V_{\beta s} \end{bmatrix} \qquad (4)$$

and (2) for flux observation is transformed into

$$\begin{bmatrix} \dot{\hat{\lambda}}_{\alpha r} \\ \dot{\hat{\lambda}}_{\beta r} \end{bmatrix} = -\begin{bmatrix} \psi_{\alpha r} \\ \psi_{\beta r} \end{bmatrix}, \qquad (5)$$

where

$$\psi_{\alpha r} = -u_0\, sign(s_{\alpha s}), \qquad \psi_{\beta r} = -u_0\, sign(s_{\beta s}), \qquad (6)$$
$$sign(s_{\alpha\beta}) = \begin{cases} 1 & \text{if } s_{\alpha\beta} > 0, \\ -1 & \text{if } s_{\alpha\beta} < 0. \end{cases}$$

and

$$\begin{aligned}
s_{\alpha s} &= \overline{I}_{\alpha s} = \hat{I}_{\alpha s} - I_{\alpha s} \\
s_{\beta s} &= \overline{I}_{\beta s} = \hat{I}_{\beta s} - I_{\beta s}. \qquad (7)
\end{aligned}$$

The sliding mode surface is defined as

$$s_n = [\, s_{\alpha s} \quad \mathbf{s}_{\beta s}\,]^T. \qquad (8)$$

$\hat{I}_{\alpha s}$, $\hat{I}_{\beta s}$ and $I_{\alpha s}$, $I_{\beta s}$ are the observed and measured stator current components, respectively.

When the estimation error trajectories reach the sliding surface ($S_n = 0$), the observed currents in (7) will converge to the actual currents ($\hat{I}_{\alpha s} = I_{\alpha s}$ and $\hat{I}_{\beta s} = I_{\beta s}$). The selection of u_0 in (6), which guarantees the current observation convergence by the Lyapunov stability analysis, is presented in the Appendix. As indicated by (5), once the estimated current converges to the measured one, the flux estimation is a mere integration of the sliding mode functions without requiring any knowledge of the rotor time constant and rotor speed. Equations (3)–(7) form the core of the current and flux observers. The block diagram for overall sliding mode observer along with the speed estimator is shown in Fig. 1.

As indicated by (6) and (7), two independent sliding mode functions, $\psi_{\alpha r}$ and $\psi_{\beta r}$, are designed for the α and β axes current observers respectively. These sliding mode functions are based on the error between the measured and estimated phase

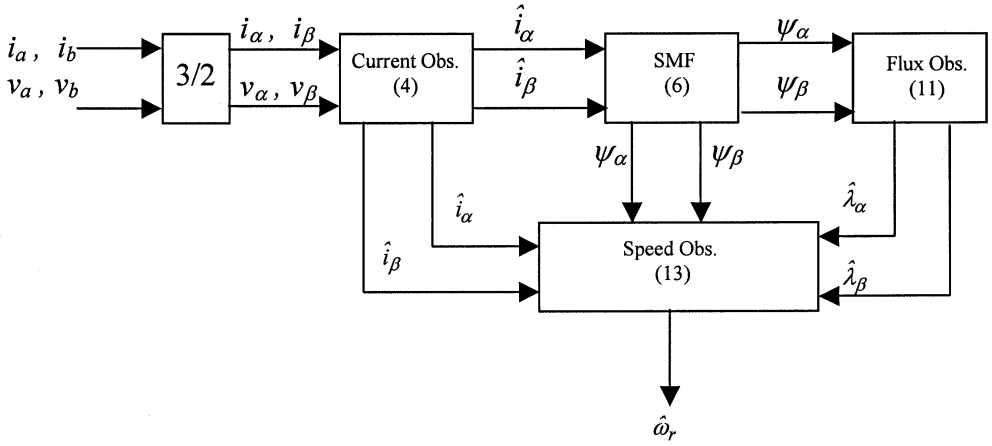

Fig. 1. Sliding mode flux and speed observer block diagram.

currents. It is important to notice that in real machine equations, there exists a coupling between the α and β axes of the current and flux equations. Especially in (2), the flux along α axis is a function of flux along β axes and vice versa. However, when the sliding mode functions defined in (6) are substituted in the observer equations, the current and flux observer models become relatively decoupled along α and β axes. This is because with these sliding mode functions, the α and β axes currents are estimated based on their self current errors (i.e., the error between the observed and measured current). The close loop current observer uses the measured current for feedback and no integration operation is used for current estimation. As a result, there is no offset or drift problem in the current observer.

B. Flux, Speed and Rotor Time Constant Estimation

As defined by (5), flux can be estimated by integration of $\psi_{\alpha r}$ and $\psi_{\beta r}$. However, $\psi_{\alpha r}$ and $\psi_{\beta r}$ will take the extreme values of u_0 and $-u_0$ at a high frequency and will oscillate around their actual values. To define the control action which maintains the motion on the sliding manifold, an "equivalent control" concept [22] is used. Solving $\dot{s}_n = 0$ for $\psi_{\alpha r}$ and $\psi_{\beta r}$ will yield the equivalent control action. In practice, the discontinuous control can be considered as a combination of an equivalent control term and a high frequency switching term. So the equivalent control term can be found by isolating the continuous term using a low-pass filter, which is implemented as

$$\psi_{\alpha\beta r}^{eq} = \frac{1}{\mu s + 1}\,\psi_{\alpha\beta r} \tag{9}$$

where μ is the time constant of the filter and is selected as 0.002. It should be sufficiently small to preserver the slow component undistorted but large enough to eliminate the high frequency components. The ripple of speed can be reduced by increasing the value of μ. Another low pass filter with a small cutoff frequency (10 to 20 Hz) can be used in the speed feedback loop to smooth the speed. When the trajectories of system reach the sliding surface $s_n = 0$, the observer currents $\hat{I}_{\alpha s}$, $\hat{I}_{\beta s}$ match the actual currents $I_{\alpha s}$, $I_{\beta s}$. Equations (3) and (9) can then be used to obtain

$$\begin{bmatrix}\psi_{\alpha r}^{eq}\\ \psi_{\beta r}^{eq}\end{bmatrix} = \left(\begin{bmatrix}\eta & \hat{\omega}_r\\ -\hat{\omega}_r & \eta\end{bmatrix}\begin{bmatrix}\hat{\lambda}_{\alpha r}\\ \hat{\lambda}_{\beta r}\end{bmatrix} - \eta L_m\begin{bmatrix}\hat{I}_{\alpha s}\\ \hat{I}_{\beta s}\end{bmatrix}\right). \tag{10}$$

Using (5) and (10), the rotor flux can be calculated as

$$\begin{bmatrix}\dot{\hat{\lambda}}_{\alpha r}\\ \dot{\hat{\lambda}}_{\beta r}\end{bmatrix} = -\begin{bmatrix}\psi_{\alpha r}^{eq}\\ \psi_{\beta r}^{eq}\end{bmatrix}. \tag{11}$$

The flux estimate from (5) or (11) can be destabilized by a variety of errors, including DC offset, parameter detuning and digital approximation errors. Therefore, a small amount of feedback is required to maintain the stability of the integral in the presence of noise or offset errors. Here, an integral scheme with a small amount of negative feedback to pure integral, which is discussed in detail in [27], [28], is used to achieve successful integration of flux equations. Next multiplying row one of (10) by $\hat{\lambda}_{\beta r}$ and row two by $\hat{\lambda}_{\alpha r}$, we obtain

$$\begin{bmatrix}\hat{\lambda}_{\beta r}\psi_{\alpha r}^{eq}\\ \hat{\lambda}_{\alpha r}\psi_{\beta r}^{eq}\end{bmatrix} = \left(\begin{bmatrix}\hat{\lambda}_{\beta r}\eta & \hat{\lambda}_{\beta r}\hat{\omega}_r\\ -\hat{\lambda}_{\alpha r}\hat{\omega}_r & \hat{\lambda}_{\alpha r}\eta\end{bmatrix}\begin{bmatrix}\hat{\lambda}_{\alpha r}\\ \hat{\lambda}_{\beta r}\end{bmatrix} - \eta L_m\begin{bmatrix}\hat{\lambda}_{\beta r}\hat{I}_{\alpha s}\\ \hat{\lambda}_{\alpha r}\hat{I}_{\beta s}\end{bmatrix}\right). \tag{12}$$

From (12) the estimated speed can be written as

$$\hat{\omega}_r = \frac{\hat{\lambda}_{\beta r}\psi_{\alpha r}^{eq} - \hat{\lambda}_{\alpha r}\psi_{\beta r}^{eq} - \eta L_m\left(\hat{I}_{\beta r}\hat{\lambda}_{\alpha r} - \hat{I}_{\alpha r}\hat{\lambda}_{\beta r}\right)}{\hat{\lambda}_{\alpha r}^2 + \hat{\lambda}_{\beta r}^2}. \tag{13}$$

Note that the rotor time constant and estimated speed are not used for the current and flux estimations. Thus an error in the rotor time constant and estimated speed will not be fed back into the current and flux estimations. The proposed algorithm is then implemented on an indirect filed oriented drive system. Synchronous speed is calculated by adding the command slip speed and the estimated rotor electrical speed. The overall system diagram is shown in Fig. 2. The details of sliding mode flux and speed observer block are already described in Fig. 1.

III. Simulation Results

Computer simulations have been developed using a 5 HP induction machine, which is also used for experimental verification in the lab, to validate the proposed algorithm for current, flux and speed estimations. The machine parameters are:

220 volts	14.8 amps	5 hp
$L_{ls} = L_{lr} = 1.9$ mh	$L_m = 41.2$ mh	1750 rpm
$R_s = 0.6$ ohms	$R_r = 0.41$ ohms	4 poles.

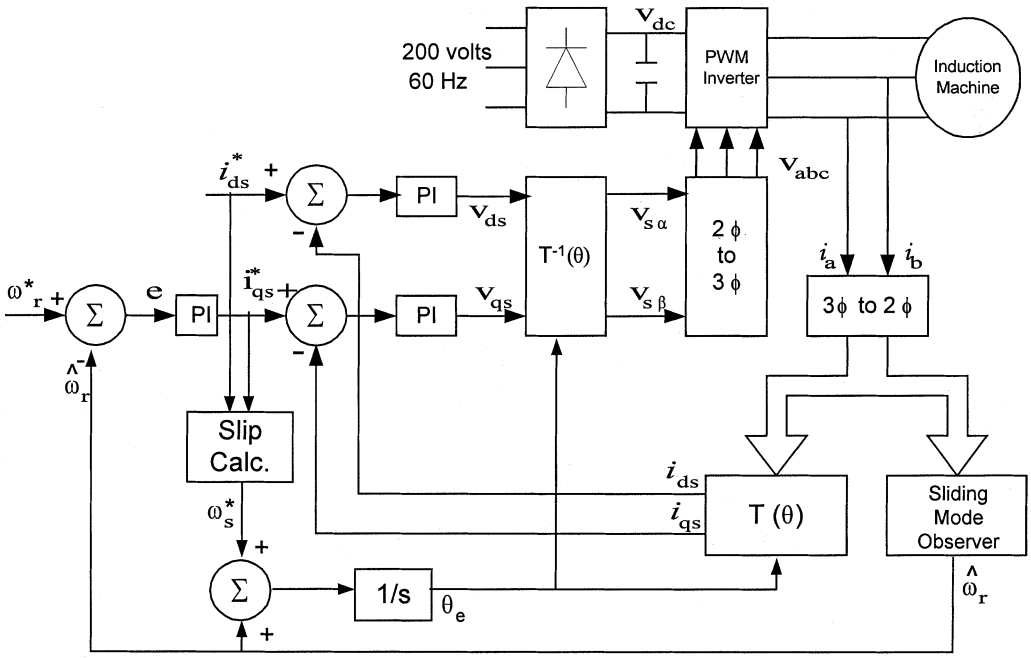

Fig. 2. Overall control system simulation and implementation block diagram.

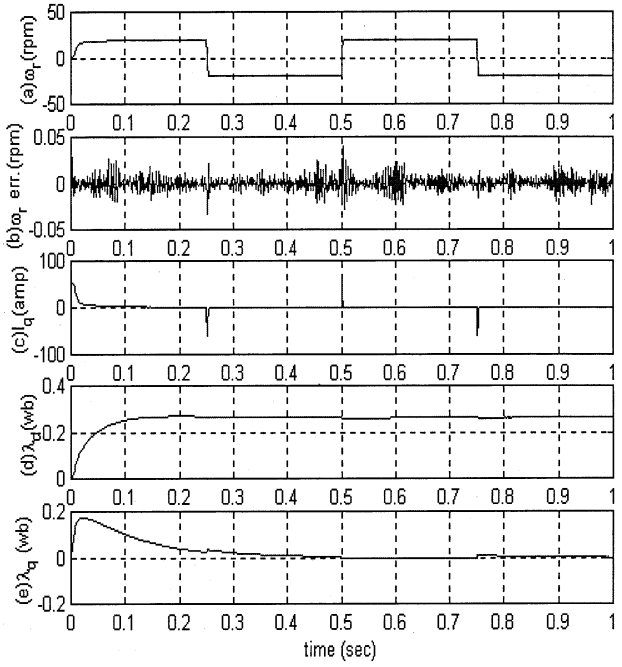

Fig. 3. Simulation results for ±20 rpm step command under no load condition.

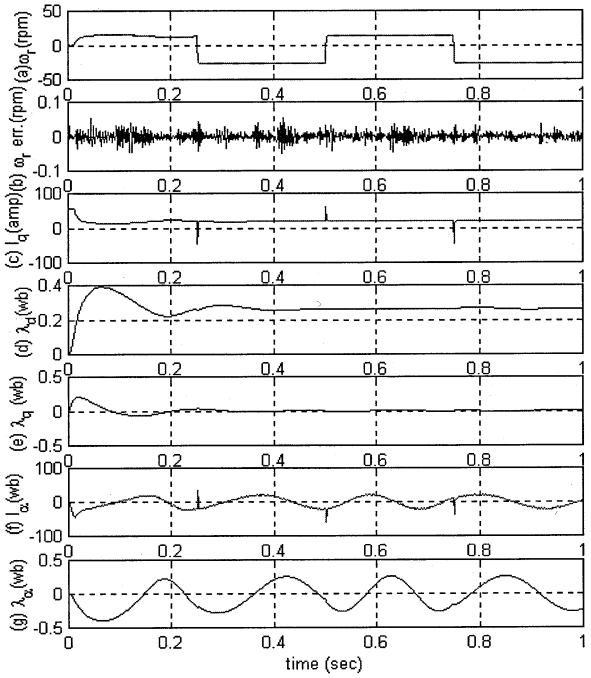

Fig. 4. Simulation results for ±20 rpm step command under full load condition.

Figs. 3 and 4 show the induction machine step response to a command of ±20 rpm under no load and full load conditions respectively. In these simulation and experimental results as well, the subscripts d–q represent the currents and fluxes in the synchronous frame and α–β show these quantities in the stationary frame of reference. The estimated speed is fed back in the closed loop for speed regulation, and a PI controller is used in the speed regulation loop. The actual machine model is used to calculate the current, flux and speed of the machine. The observer model described in Section II is used to estimate these quantities. The actual and estimated speeds, currents and fluxes are plotted on top of each other to illustrate the algorithm performance. In Figs. 3 and 4, trace (a) shows the actual and estimated speed, and trace (b) shows the error between the actual and estimated speed. Trace (c) represents the q-axis current, and the actual and estimated fluxes along d and q axis are presented in the trace (d) and trace (e) respectively. In addition, Fig. 4 trace (f) and (g), show the actual and estimated current and flux along the α axis in the stationary frame for full load condition.

These simulation results substantiate the expected performance of the proposed algorithm. The estimated machine

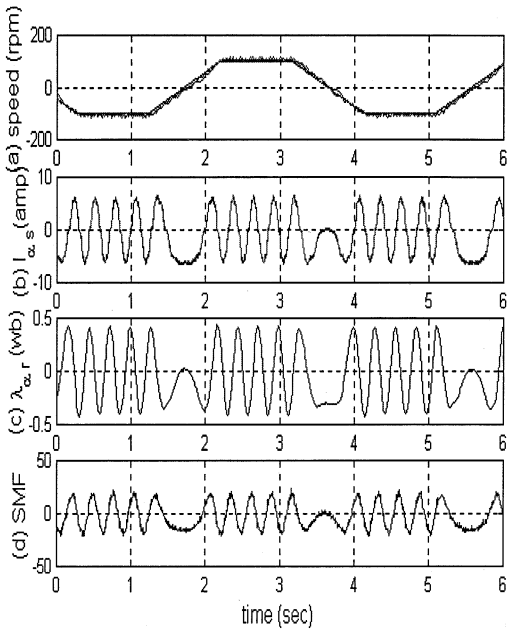

Fig. 5. Experimental results for a 100 rpm trapezoidal speed command.

currents and fluxes converge to real values very quickly for no load and full load conditions. Thus, the estimated speed converges to the actual speed. The error between the estimated and measured speed is less than 0.1 rpm [Figs. 3 and 4 trace (b)] at any time, proving that the observer performance is quite satisfactory both under no load and full load conditions.

IV. Experimental Results

The experimental test setup consists of a 5 HP cage induction motor, an IGBT inverter, and a flexible high performance Advanced Controller for Electric Machine (ACE) [29]. The DSP on the CPU board performs all real time control functions while a microprocessor performs downloading, data logging, and data communication functions. The proposed algorithm has been extensively tested using this test setup, for a wide speed range and various speed signals. The performance is also evaluated under an external disturbance, and with parameter variation. The results are summarized in this section.

A. Performance Over Wide Speed Range With Various Speed Command Signals

Various tests are conducted to characterize the performance of the proposed algorithm. Fig. 5 shows the observer performance for a 100 rpm (about $\pm 5\%$ of rated speed) trapezoidal reference speed using the proposed sensorless algorithm. The trapezoidal reference speed is chosen so that the induction machine under testing experiences both motoring and generating modes of operation, rotating in both directions at variable and constant speeds. The sliding mode function [trace (d)] drives the estimated current to the measured one. Once the estimated current converges to the measured one, flux is obtained by integration of the sliding mode function. The estimated flux is plotted in trace (c). The accuracy of the flux estimation is reflected both in the speed plot, trace (a), and in the current plot, trace (b). In trace (a) the command, estimated and actual speed measured through the encoder are plotted on top of each other. The error between the speed measured through encoder and the estimated speed is about 3 to 5%. Thus the observer proved to estimate the speed correctly, validating the overall control system performance. Note that the algorithm is made fully sensorless by using the estimated speed for speed regulation, and calculating the synchronous speed by adding the command slip and the estimated rotor speed (algorithm is implemented in IFO). The integrated data acquisition capability of the ACE proved quite handy to collect these eight different signals simultaneously.

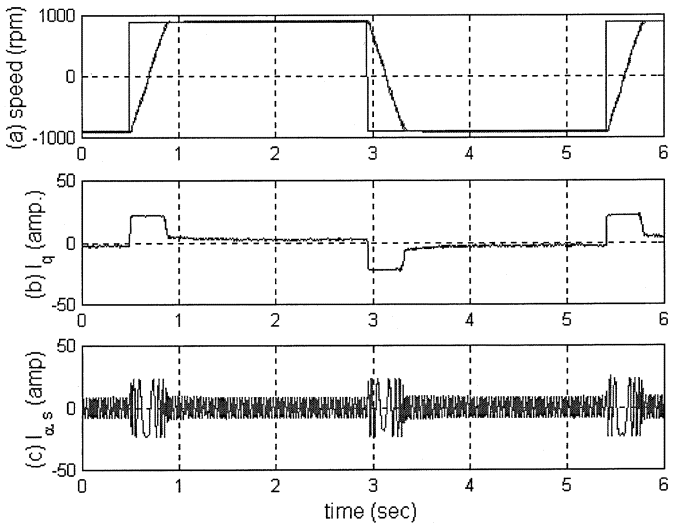

Fig. 6. Experimental results for a ± 900 rpm step wave speed command tracking.

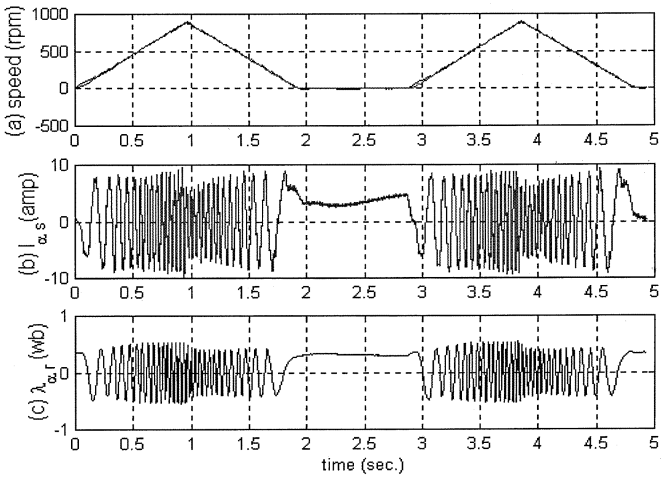

Fig. 7. Experimental results for a 900 rpm triangular speed tracking.

Next experiments are performed for step, triangular, and trapezoidal speed references to verify the algorithm performance at sharp changes in speed, variable and constant speed over wide speed range. In Fig. 6 the transient step speed response includes the command, actual and estimated speeds [trace (a)], the torque current I_q [trace (b)] and the phase current [trace (c)] have been plotted. The triangular wave speed tracking response, Fig. 7, includes the speed [trace (a)], phase current [trace (b)] and flux [trace (c)]. Fig. 6 clearly demonstrates that the sensorless control performance to the step speed change from -900 to $+900$ rpm is very satisfactory.

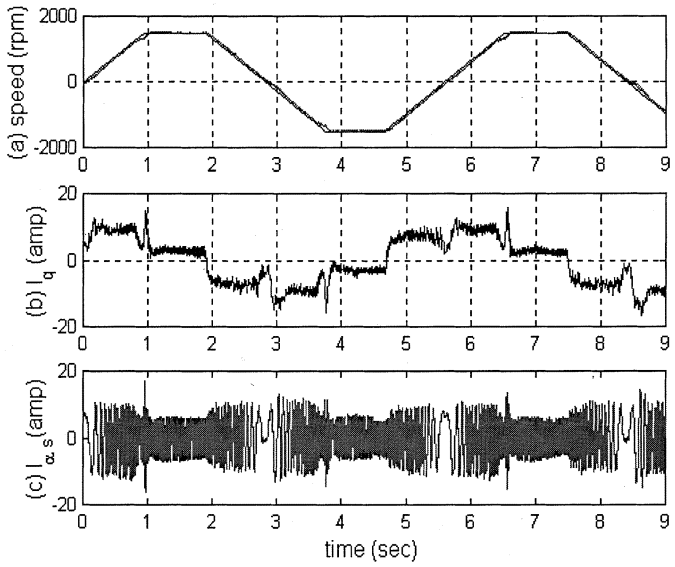

Fig. 8. Experimental results for 1500 rpm trapezoidal speed command.

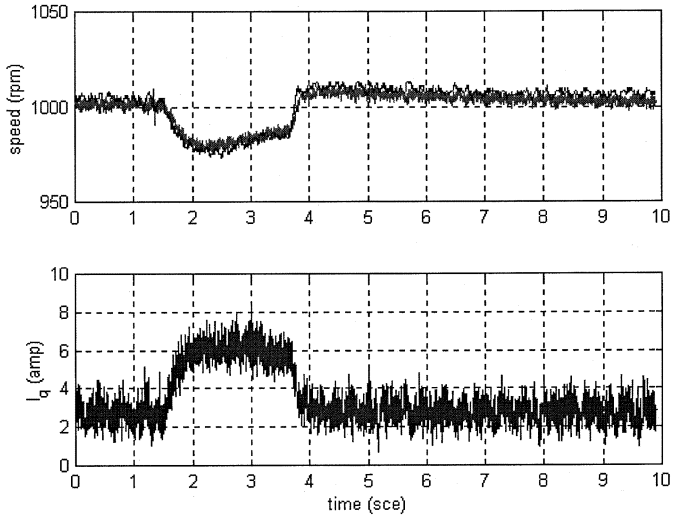

Fig. 9. Experimental results under external disturbance.

In Fig. 7, the triangular wave speed tracking demonstrates the observer performance at very sharp corners of the speed transition. Finally, Fig. 8 shows the testing results for a 1500 rpm trapezoidal speed reference for 4-quadrant operation, thus completing the tests over a wide speed range with various command signals.

B. Observer Performance Under External Disturbance

The observer sensitivity to an external load disturbance is investigated in this section. The machine is initially set to operate at 1000 rpm in steady state. A sudden load is then applied to the motor shaft for a short period of time. As a result, the rotor speed under this disturbance dips to about 980 rpm, a decrease of approximately 2%. This speed dip is due to the PI based speed regulator. However, all observers can sense this sudden load disturbance in speed, and act accordingly to maintain the sensorless field orientation control of the induction machine as can be seen in Fig. 9.

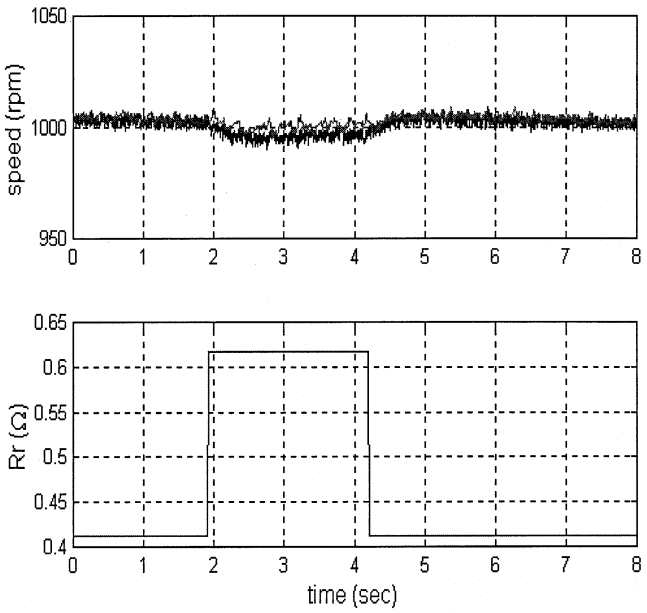

Fig. 10. Experimental results under rotor resistance variation.

C. Parameter Variation Effect

The designed observer is robust because of the nature of underlying sliding mode technique and a close loop observer. As discussed in the theoretical analysis, the parameters replaced by the sliding mode functions do not affect the observer performance at all. For instance, the error in the estimated speed does not affect the current and flux estimations. Likewise, an error in the rotor time constant will not affect the observed current and flux either.

One common parameter that varies with the temperature is the rotor time constant. In this test machine is maintained at steady state 1000 rpm and is operated with its nominal rotor time constant. At certain moment the rotor resistance setting of the observer is suddenly set to 1.5 times of its nominal value in the controller, which virtually changes the rotor time constant by 50%. Fig. 10 shows the results as this change is applied to the observer. The estimated speed varies by less than 1% under these conditions (estimated: $\sim$992 rpm, measured: $\sim$1000 rpm). This proves that the proposed speed estimation is robust under rotor time constant variation without employing any on-line rotor time constant compensation.

V. Conclusion

This paper successfully developed a new current model flux observer for speed sensorless control of induction machines. Based on the simulations and experimental results, the proposed current, rotor flux and rotor speed observers exhibit the following salient features.

1) The proposed algorithm works very well under transient as well as steady state conditions over wide speed range, (from $\pm$5% to $\pm$100% of rated speed).
2) The current and flux observers do not require any knowledge of the machine speed or rotor time constant because they are absorbed into the sliding mode functions. Thus, the proposed flux observer is not sensitive to any error

in speed information or rotor resistance variation, problems commonly associated with the current model flux observer. Speed estimation requires the rotor time constant. However, variation in the rotor time constant has little effect on the estimated speed.

3) The algorithm is simple to implement and is not computationally intensive.

APPENDIX

A. Lyapunov Stability Analysis for the Proposed Observer

The stability of the overall observer structure is guaranteed through the stability analysis of the current observer. The Lyapunov function for the proposed sliding mode current observer is chosen as

$$V = \tfrac{1}{2}\, s_n^T s_n$$

where $s_n = [s_{\alpha s} \;\; s_{\beta s}]^T$. The Lyapunov function V is positive definite. This satisfies the first Lyapunov stability condition. The second condition is that the derivative of the sliding mode functions must be less than zero i.e., $\dot{V} = s_n^T \dot{s}_n < 0$ with

$$s_n = \begin{bmatrix} \overline{I}_{\alpha s} \\ \overline{I}_{\beta s} \end{bmatrix}, \qquad \dot{s}_n = \begin{bmatrix} \dot{\overline{I}}_{\alpha s} \\ \dot{\overline{I}}_{\beta s} \end{bmatrix}.$$

Using (1) and (4), $\dot{s}_n$ can be written as

$$\dot{s}_n = k_1 \left(\begin{bmatrix} \psi_{\alpha r} \\ \psi_{\beta r} \end{bmatrix} - \begin{bmatrix} \eta & \omega_r \\ -\omega_r & \eta \end{bmatrix} \begin{bmatrix} \lambda_{\alpha r} \\ \lambda_{\beta r} \end{bmatrix} + \eta L_m \begin{bmatrix} I_{\alpha s} \\ I_{\beta s} \end{bmatrix} \right) - k_2 \begin{bmatrix} \overline{I}_{\alpha s} \\ \overline{I}_{\beta s} \end{bmatrix}.$$

Therefore

$$\dot{V} = k_1 \left[\overline{I}_{\alpha s} \quad \overline{I}_{\beta s} \right] \left(\begin{bmatrix} -u_0\, sign\left(\overline{I}_{\alpha s}\right) \\ -u_0\, sign\left(\overline{I}_{\beta s}\right) \end{bmatrix} - \begin{bmatrix} \eta & \omega_r \\ -\omega_r & \eta \end{bmatrix} \times \begin{bmatrix} \lambda_{\alpha r} \\ \lambda_{\beta r} \end{bmatrix} - \eta L_m \begin{bmatrix} I_{\alpha s} \\ I_{\beta s} \end{bmatrix} \right) - k_2 \left[\overline{I}_{\alpha s} \quad \overline{I}_{\beta s} \right] \begin{bmatrix} \overline{I}_{\alpha s} \\ \overline{I}_{\beta s} \end{bmatrix}.$$

This implies that $\dot{V} < 0$ if

$$u_0 > \frac{\left| \overline{I}_{\alpha s} A + \overline{I}_{\beta s} B \right| - \frac{k_2}{k_1} \left(\left(\overline{I}_{\alpha s}\right)^2 + \left(\overline{I}_{\beta s}\right)^2 \right)}{\left| \overline{I}_{\alpha s} \right| + \left| \overline{I}_{\beta s} \right|} \tag{14}$$

where

$$A = \eta \lambda_{\alpha r} + \omega_r \lambda_{\beta r} + \eta L_m I_{\alpha s},$$
$$B = \eta \lambda_{\beta r} - \omega_r \lambda_{\alpha r} + \eta L_m I_{\beta s}.$$

By selecting a large enough u_0 found by the existence condition above, the convergence of the current observer can be guaranteed. The selection of u_0 in real implementation is quite trivial. This is because even though u_0 has a bound on its minimum value defined by (14), there is no restriction on its upper limit. Therefore, it can be tuned very easily for satisfactory current convergence.

REFERENCES

[1] R. M. Cuzner, R. D. Lorenz, and D. W. Novotny, "Application of nonlinear observers for rotor position detection on an induction motor using machine voltages and currents," in *Proc. IEEE-IAS Annu. Meeting Conf.*, Oct. 1990, pp. 416–421.

[2] A. Ferrah, K. G. Bradely, and G. M. Asher, "Sensroless speed detection of inverter fed induction motors using rotor slot harmonics and fast Fourier transform," in *Proc. IEEE-PESC Conf.*, Oct. 1992, pp. 279–286.

[3] J. Cilia, G. M. Asher, K. J. Bradley, and M. Sumner, "Sensorless position detection for vector-controlled induction motor drives using an asymmetric outer-section cage," *IEEE Trans. Ind. Applicat.*, vol. 33, pp. 1162–1169, Sept./Oct. 1997.

[4] P. L. Jansen and R. D. Lorenz, "Transducerless position and velocity estimation in induction and salient AC machines," *IEEE Trans. Ind. Applicat.*, vol. 31, pp. 240–247, Mar./Apr. 1995.

[5] ——, "Transducerless field orientation concepts employing saturation-induced saliencies in induction machines," *IEEE Trans. Ind. Applicat.*, vol. 32, pp. 1380–1393, Nov./Dec. 1996.

[6] F. Blaschke, J. Van der burget, and A. Vandenput, "Sensorless direct field orientation control at zero flux frequency," in *Proc. IEEE-IAS Annu. Meeting Conf.*, San Diego, CA, Oct. 1996, pp. 189–196.

[7] N. Teske, G. M. Asher, M. Sumner, and K. J. Bradley, "Suppression of saturation saliency effects for the sensorless position control of induction motor drives under loaded conditions," *IEEE Trans. Ind. Applicat.*, vol. 47, pp. 1142–1150, Sept./Oct. 2000.

[8] ——, "Encoderless position estimation for symmetric cage induction machines under loaded conditions," *IEEE Trans. Ind. Applicat.*, vol. 37, pp. 1793–1800, Nov./Dec. 2001.

[9] R. Gabriel, W. Leonhard, and C. Nordby, "Field oriented control of standard AC motor using microprocessor," *IEEE Trans. Ind. Applicat.*, vol. IA-16, pp. 186–192, 1980.

[10] X. Xu and D. W. Novotny, "Implementation of direct stator flux orientation control on a versatile DSP based system," *IEEE Trans. Ind. Applicat.*, vol. 27, pp. 694–700, July/Aug. 1991.

[11] X. Xu, R. De Doncker, and D. W. Novotny, "A stator flux oriented induction machine drive," in *Proc. IEEE-PESC Conf.*, vol. 2, Apr. 1988, pp. 870–876.

[12] ——, "Stator flux orientation control of induction machines in the field weakening region," in *Proc. IEEE-IAS Annu. Meeting Conf.*, Oct. 1988, pp. 437–443.

[13] P. L. Jansen and R. D. Lorenz, "A physical insightful approach to the design and accuracy assessment of flux observers for field oriented induction machine drives," *IEEE Trans. Ind. Applicat.*, vol. 30, pp. 101–110, Jan./Feb. 1994.

[14] P. L. Jansen, R. D. Lorenz, and D. W. Novotny, "Observer-based direct field orientation: Analysis and comparison of alternative methods," *IEEE Trans. Ind. Applicat.*, vol. 30, pp. 945–953, July/Aug. 1994.

[15] G. C. Vershese and S. R. Sanders, "Observers for flux estimation in induction machines," *IEEE Trans. Ind. Electron.*, vol. 35, pp. 85–94, Feb. 1988.

[16] H. Tajima and Y. Hori, "Speed sensorless field-orientation control of the induction machine," *IEEE Trans. Ind. Applicat.*, vol. 29, pp. 175–180, Jan./Feb. 1993.

[17] F.-Z. Peng and T. Fukao, "Robust speed identification for speed-sensorless vector control of induction motors," *IEEE Trans. Ind. Applicat.*, vol. 30, pp. 1234–1240, Sept./Oct. 1994.

[18] L. Zhen and L. Xu, "A mutual MRAS identification scheme for position sensorless field orientation control of induction machines," in *Proc. IEEE-IAS Annu. Meeting Conf.*, Orlando, FL, Oct. 1995, pp. 159–165.

[19] L. Harnefors, "Design and analysis of general rotor-flux oriented vector control systems," *IEEE Trans. Ind. Electron.*, vol. 48, pp. 383–389, Apr. 2001.

[20] Y. R. Kim, S. K. Sul, and M. Park, "Speed sensorless vector control of induction motor by using extended Kalman filter," *IEEE Trans. Ind. Applicat.*, vol. 30, pp. 1225–1233, Sept./Oct. 1994.

[21] Y. S. Kim, S. U. Kim, and L. W. Yang, "Implementation of a speed sensorless vector control of induction machine by reduced-order Kalman filter," in *Proc. IEEE APEC 95 Conf.*, Dallas, TX, Mar. 1995, pp. 197–203.

[22] V. I. Utkin, "Sliding mode control design principles and applications to electric drives," *IEEE Trans. Ind. Electron.*, vol. 40, pp. 23–36, Feb. 1993.

[23] Z. Yan, C. Jin, and V. I. Utkin, "Sensorless sliding-mode control of induction motors," *IEEE Trans. Ind. Electron.*, vol. 47, pp. 1286–1297, Dec. 2000.

[24] F. Parasiliti, R. Petrella, and M. Tursini, "Adaptive sliding mode observer for speed sensorless control of induction motors," in *Proc. IEEE-IAS Annu. Meeting Conf.*, 1999, pp. 2277–2283.

[25] A. Benchaib, A. Rachid, and E. Auderzet, "Sliding mode input–output linearization and field orientation for real-time control of induction motors," *IEEE Trans. Ind. Electron.*, vol. 14, pp. 3–13, Jan./Feb. 1999.
[26] A. Benchaib, A. Rachid, E. Auderzet, and M. Tadjine, "Real-time sliding-mode observer and control of an induction motor," *IEEE Trans. Ind. Electron.*, vol. 46, pp. 128–138, Feb. 1999.
[27] K. D. Hurst, T. G. Habetler, G. Griva, and F. Profumo, "Zero-speed tacholess IM torque control: Simply a matter of stator voltage integration," *IEEE Trans. Ind. Applicat.*, vol. 34, pp. 790–794, July 1998.
[28] J. Hu and B. Wu, "New integration algorithms for estimating motor flux over a wide speed range," *IEEE Trans. Power Electron.*, vol. 13, pp. 969–977, Sept. 1998.
[29] H. Rehman and R. J. Hampo, "A flexible high performance advanced controller for electric machines," in *Proc. IEEE APEC'00 Conf.*, St. Louis, MO, Feb. 2000, pp. 939–943.

Habib ur Rehman (M'01) received the B.Sc. degree in electrical engineering from the University of Engineering and Technology, Lahore, Pakistan, in 1990 and the M.S. and Ph.D. degrees in electrical engineering from the Ohio State University, Columbus, in 1995 and 2001, respectively.

He worked in the Ecostar Electric Drives and Ford Research Laboratory as a Design Engineer, from July 1998 to December 1999. He was involved in the Electric, Hybrid, and Fuel Cell Vehicles Development Programs. He joined the Department of Electrical Engineering, United Arab Emirates University, Al-ain, in 2001 as an Assistant Professor. His primary research interests are in the areas of microprocessor/digital signal processor based adjustable-speed drives, fuzzy logic, and sliding mode control applications to drives. Presently, he is working on the observers development for direct/indirect field oriented motor drives with/without sensor.

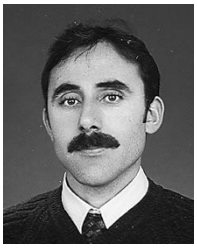

Adnan Derdiyok was born in Horasan, Turkey, on December 12, 1964. He received the B.S. degree in electrical engineering from Technical University of Istanbul, in 1988, the M.S. degree from Middle East Technical University, in 1993, and the Ph.D. degree from Yıldız Technical University, Turkey, in 1997.

Since 1997, he has been with Atatürk University, Erzurum, Turkey, where he is an Associate Professor. In 2000, he was with the Ohio State University, Columbus, where he was engaged in post-doctoral research and development of sensorless control techniques for induction machine. His research interests include control of electrical machines, sensorless control of induction machine, modeling and control of switched reluctance motor, fuzzy, and sliding mode control techniques.

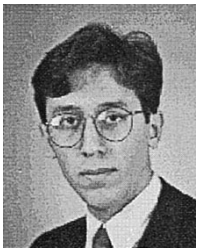

Mustafa K. Güven (M'02) received the B.Sc. degree in electrical engineering from Istanbul Technical University, Istanbul, Turkey, in 1993 and the M.S. and Ph.D. degrees in electrical engineering from the Ohio State University, Columbus, in 1997 and 2001, respectively.

He has been working for Caterpillar, Inc. as a Senior Research Engineer since September 2001. His research interests include advance control theory, digital signal processors, and their applications in controlling motion systems.

Longya Xu (S'89–M'90–SM'93) received the M.S. and Ph.D. degrees from the University of Wisconsin, Madison, in 1986 and 1990, respectively, both in electrical engineering.

He joined the Department of Electrical Engineering, Ohio State University, Columbus, in 1990, where he is presently a Professor. He has served as a Consultant to many industry companies including Raytheon Company, U.S. Wind Power Company, General Motors, Ford Motor, and Unique Mobility, Inc. for various industrial concerns.

His research and teaching interests include dynamic modeling and optimized design of electrical machines and power converters for variable speed generating and drive system, application of advanced control theory and digital signal processor in controlling of motion systems for super-high speed operation.

Dr. Xu received the 1990 First Prize Paper Award in the Industry Drive Committee, IEEE/IAS, the Research Initiation Award from National Science Foundation in 1991, and the 1995 and 1999 Lumley Research Award for his outstanding research accomplishments from College of Engineering, The Ohio State University. He currently serves as the Chairman of Electric Machine Committee of IEEE/IAS and an Associate Editor of the IEEE TRANSACTIONS ON POWER ELECTRONICS.